

Nuclear Production and Analytic Attenuation of Energetic MeV Solar Dark Matter

Shao-Feng Ge,^{1, 2, *} Jie Sheng,^{1, 2, †} Chen Xia,^{1, 2, 3, ‡} and Chuan-Yang Xing^{1, 2, 4, §}

¹*State Key Laboratory of Dark Matter Physics, Tsung-Dao Lee Institute & School of Physics and Astronomy, Shanghai Jiao Tong University, Shanghai 200240, China*

²*Key Laboratory for Particle Astrophysics and Cosmology (MOE) & Shanghai Key Laboratory for Particle Physics and Cosmology, Shanghai Jiao Tong University, Shanghai 200240, China*

³*Shanghai Synchrotron Radiation Facility, Shanghai Advanced Research Institute, Chinese Academy of Sciences, Shanghai 201204, China*

⁴*College of Science, China University of Petroleum (East China), Qingdao 266580, China*

We propose a solar production mechanism of MeV dark matter to overcome the energy threshold in direct detection experiments. In particular, the proton and deuteron fusion to ${}^3\text{He}$ of the pp chain that produces energetic neutrino and gamma photon with 5.5 MeV of energy release can also produce a pair of dark matter particles. Besides, we establish an analytical formalism of using the Boltzmann equation to study the solar attenuation effect on the produced dark matter flux. The projected sensitivity is illustrated with Argon target at the DarkSide-LowMass experiment.

I. Introduction

There are ample evidences of the existence of dark matter (DM) from cosmological and astrophysical observations [1–4]. The current direct detection experiments are sensitive to DM with mass $\gtrsim \mathcal{O}(\text{GeV})$ [5]. In particular, the most stringent sensitivity on the spin-independent DM-nucleon scattering cross section σ_{SI} reaches $\mathcal{O}(10^{-47}) \text{ cm}^2$ [6–8]. On the other hand, the sub-GeV mass range is much less constrained with not enough energy to overcome the recoil energy threshold.

Various new detection approaches with lower detection thresholds have been proposed to increase the sensitivity for light DM, including the Bremsstrahlung [9] and Migdal [10–13] effects, fermionic absorption [14–19] and nucleon consumption [20, 21] scenarios, as well as new detection materials [22–26]. In addition, new sources of energetic DM can also help to overcome the detection threshold. For example, DM can be boosted by semi-annihilation [27, 28], cosmic rays [29–46], blazars [47, 48], the nearest active galactic nucleus Centaurus A [49], cosmic and supernova neutrinos [50–54], solar reflection [55–57], etc. Besides boosting the existing DM particles, their decay [58, 59] or annihilation [60] can produce relativistic dark particles. In addition, boosted dark particles can also evaporate from black holes [61] or appear in the cosmic ray dump in the Earth atmosphere [62–65].

Those boosting mechanisms are all related to astrophysical or atmospheric processes or origins. Of them, the solar reflection with acceleration by thermal electrons inside Sun can only be measured by the electron recoil signal. Corresponding to a typical temperature around 15 million kelvins, the energy is in the $\mathcal{O}(\text{keV})$ range which

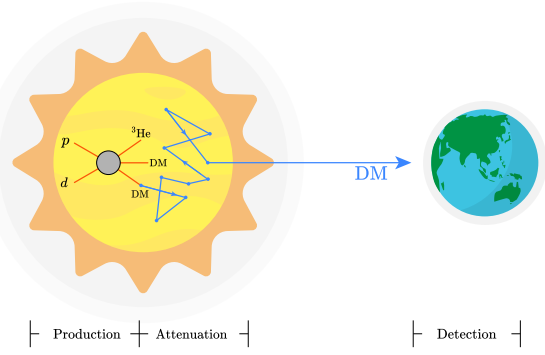


FIG. 1. Schematic illustration of the production, attenuation and detection of energetic solar DM.

is still far from overcoming the detection threshold with nuclei recoil. However, the nuclear fusion inside Sun is intrinsically at the $\mathcal{O}(\text{MeV})$ scale. The corresponding energy release is large enough to produce energetic DM and subsequently nuclei recoil above the detection threshold.

We propose a possible way of producing energetic MeV DM from the solar pp chain to overcome the direct detection threshold with nuclei recoil. Fig. 1 sketches the three key processes, 1) the production of MeV DM from the solar pp chain, 2) the DM scattering with nuclei and the resultant solar attenuation, 3) the DM direct detection on our Earth, to be elaborated below.

II. MeV Solar Dark Matter Production from pp Chain

Although the solar nuclear fusion process contains both pp chain and CNO cycle [66], the latter contributes only 1% to the energy production and hence can be ignored. There are three photon emission processes in the pp chain. Of them, $p + {}^7\text{Be} \rightarrow {}^8\text{B} + \gamma$ contributes less than 1%. Though ${}^3\text{He} + {}^4\text{He} \rightarrow {}^7\text{Be} + \gamma$ has a sizable branching ratio

* Corresponding Author: gesf@sjtu.edu.cn

† shengjie04@sjtu.edu.cn

‡ xiac@sari.ac.cn

§ Corresponding Author: cyxing@upc.edu.cn

of 16.7%, the released energy of 1.6 MeV is not enough to overcome the nuclear recoil detection threshold. Only the fusion of proton (p) with deuteron (d), $p+d \rightarrow {}^3\text{He}+\gamma$, has large enough branching ratio (100%) and energy release at 5.5 MeV [66]. So the MeV DM production is mainly through $p+d \rightarrow {}^3\text{He}+X$ where X denotes a group of DM particles. Due to stability, the DM particle usually appears in pair, $p+d \rightarrow {}^3\text{He}+\chi^*+\chi$, with $X \equiv \chi^*\chi$. We dub such DM as *Solar Dark Matter*, in the same sense as solar neutrino [67, 68] or solar axion [69–72].

The momentum transfer, same order as the 5.5 MeV released energy, corresponds to a length of 35 fm which is larger than the size of p and d . So one may neglect their internal structures. In addition, the DM production involves the scattering of p and d initial states into a bound state ${}^3\text{He}$ under the influence of Coulomb and nuclear potentials [73]. While the initial state is taken as an ionized state of the p - d system, the product ${}^3\text{He}$ is the ground state. The fusion process can then be viewed as a transition from the ionized state to the ground state [74, 75] by emitting a DM pair.

Matrix Element – We consider a simple interaction of a complex scalar DM χ and proton for illustration, $\mathcal{L} \equiv \frac{1}{\Lambda} \chi^* \chi \bar{p}p$, where Λ is a cutoff scale. Using its non-relativistic form [76, 77] for the DM coupling with the fermionic p - d system, the fusion matrix element reads,

$$T = \langle f; \mathbf{p}_{\chi^*}, \mathbf{p}_\chi | \int d^3\mathbf{x} dt \frac{i}{\Lambda} [\chi^*(\mathbf{x}_p, t) \chi(\mathbf{x}_p, t) \psi^\dagger(\mathbf{x}, t) \psi(\mathbf{x}, t) + \chi^*(\mathbf{x}_d, t) \chi(\mathbf{x}_d, t) \psi^\dagger(\mathbf{x}, t) \psi(\mathbf{x}, t)] |i\rangle, \quad (1)$$

where $\psi(\mathbf{x}, t) = \sum_n \hat{a}_n^{pd} \phi_n(\mathbf{x}) e^{-iE_n t} + \text{h.c.}$ is the second-quantized field for the p - d system [77]. The energy eigenvalue E_n and wave function ϕ_n are solved by the Schrödinger equation with the potential in Eq. (8) while \hat{a}_n^{pd} is the annihilation operator for the corresponding state. The two terms stand for the contributions from proton at \mathbf{x}_p and deuteron at \mathbf{x}_d , respectively. In the center-of-mass frame, $\mathbf{x}_p \simeq \frac{2}{3}\mathbf{x}$ and $\mathbf{x}_d \simeq -\frac{1}{3}\mathbf{x}$. Therefore, from $T \equiv (2\pi)\delta(E_\chi + E_{\chi^*} + E_f - E_i)\mathcal{M}$, we can extract the scattering amplitude,

$$\mathcal{M} = \frac{i}{\Lambda} \int d^3\mathbf{x} (e^{-i\frac{2}{3}\mathbf{q}\cdot\mathbf{x}} + e^{i\frac{1}{3}\mathbf{q}\cdot\mathbf{x}}) \phi_f^\dagger(\mathbf{x}) \phi_i(\mathbf{x}), \quad (2)$$

where the momentum transfer $\mathbf{q} \equiv \mathbf{p}_\chi + \mathbf{p}_{\chi^*}$ is the total DM momentum. The momentum transfer is smaller than the energy release (which is approximately the size of binding energy $|E_b| = 5.5$ MeV) since $|\mathbf{q}| \leq |\mathbf{p}_\chi| + |\mathbf{p}_{\chi^*}|$ and $E_\chi + E_{\chi^*} \simeq |E_b|$. Namely, $|\mathbf{q}| \lesssim |E_b| = 5.5$ MeV, and consequently the bound-state wave function is predominantly localized within the region $|\mathbf{x}| \lesssim 1/\sqrt{2m_p|E_b|} \simeq (100 \text{ MeV})^{-1}$ where m_p is the proton mass. Thus, $\mathbf{q} \cdot \mathbf{x} \lesssim 1/20$ is a small quantity for Taylor expansion. The leading order of the amplitude vanishes since the initial-state wave function $\phi_i(\mathbf{x})$ and its final-state counterpart $\phi_f(\mathbf{x})$ are orthogonal to each other. The nonzero contribution then appears at the linear order as an E1 transition,

$$\mathcal{M} \simeq \frac{1}{3\Lambda} \int d^3\mathbf{x} (\mathbf{q} \cdot \mathbf{x}) \phi_f^\dagger(\mathbf{x}) \phi_i(\mathbf{x}) \equiv \frac{1}{3\Lambda} \mathbf{q} \cdot \langle f | \mathbf{x} | i \rangle, \quad (3)$$

where $\langle f | \mathbf{x} | i \rangle \equiv \int \mathbf{x} \phi_f^\dagger(\mathbf{x}) \phi_i(\mathbf{x}) d^3\mathbf{x}$ captures the dipole structure.

Differential Cross Section – With the matrix element Eq. (3) above, the transition rate $d\Gamma_{fi}$ between the initial and final states can be obtained via the Fermi's Golden Rule [78],

$$d\Gamma_{fi} = \overline{|\mathcal{M}|^2} (2\pi) \delta(E_i - E_f - E_\chi - E_{\chi^*}) d\Phi_n, \quad (4)$$

where $d\Phi_n$ is the n -body final-state phase space,

$$d\Phi_n \equiv \frac{d^3\mathbf{p}_\chi}{(2\pi)^3 2E_\chi} \frac{d^3\mathbf{p}_{\chi^*}}{(2\pi)^3 2E_{\chi^*}}. \quad (5)$$

Note that it only contains the DM phase space. Since the final bound state f is fixed, as will be shown later, there is no continuous degree of freedom in its quantum state. Taking the matrix element in our case Eq. (3) into Eq. (4), one gets,

$$d\Gamma_{fi} = \left(\frac{1}{6} \frac{1}{9\Lambda^2} \sum_{\text{spins}} |\mathbf{q} \cdot \langle f | \mathbf{x} | i \rangle|^2 \right) (2\pi) \times \delta(E_i - E_f - E_\chi - E_{\chi^*}) \frac{d^3\mathbf{p}_\chi}{(2\pi)^3 2E_\chi} \frac{d^3\mathbf{p}_{\chi^*}}{(2\pi)^3 2E_{\chi^*}}, \quad (6)$$

where the prefactor $1/6$ comes from the average over the initial proton with spin 1/2 and deuteron with spin 1. Through the relationship between the momentum transfer and the momentum of the final-state DM particles $\mathbf{q} = \mathbf{p}_\chi + \mathbf{p}_{\chi^*}$, the integration over \mathbf{p}_{χ^*} can be transformed into the integration over \mathbf{q} . This would allow factorization of \mathbf{q} and $\langle f | \mathbf{x} | i \rangle$ by the zenith angle ($d\cos\theta_q$) integration, $\int |\mathbf{q} \cdot \langle f | \mathbf{x} | i \rangle|^2 d\cos\theta_q = 2|\mathbf{q}|^2 |\langle f | \mathbf{x} | i \rangle|^2/3$. Then the \mathbf{q} integration contains a $\int |\mathbf{q}|^4 d|\mathbf{q}|$. By using the energy conservation delta function, the integration over the angle can yield the factor $E_{\chi^*}/|\mathbf{q}||\mathbf{p}_\chi|$ since $E_{\chi^*} \equiv \sqrt{|\mathbf{q}|^2 - 2|\mathbf{q}||\mathbf{p}_\chi| \cos\theta_{|\mathbf{q}|,|\mathbf{p}_\chi|} + E_\chi^2}$. Taking this into consideration, the integration contains $\int |\mathbf{q}|^3 d|\mathbf{q}|$, and the transition rate should be proportional to $|\mathbf{q}|^4$ as,

$$\frac{d\sigma_\chi}{dE_\chi} = \frac{|\mathbf{q}|_{\max}^4 - |\mathbf{q}|_{\min}^4}{10368\pi^3 v_{pd} \Lambda^2} \sum_{\text{spins}} |\langle f | \mathbf{x} | i \rangle|^2, \quad (7)$$

where the maximal and minimal momentum transfer are defined as $|\mathbf{q}|_{\max, \min} \equiv ||\mathbf{p}_\chi| \pm |\mathbf{p}_{\chi^*}||$, and the summation is taken over all the initial and final particle spins. The factor v_{pd} in the denominator is the asymptotic relative velocity between proton and deuteron. The above differential cross section is the transition rate $d\Gamma_{fi}$ over a flux factor \mathcal{F} . Due to the interaction between the proton and deuteron, the incident wave function of the system in the center-of-mass frame is no longer a plane wave, but has the form of $\phi_i(\mathbf{x}) \sim e^{i\mathbf{k}\cdot\mathbf{x}} + f(\theta)e^{i\mathbf{k}|\mathbf{x}|}/|\mathbf{x}|$ [79], whose specific solution will be discussed in detail in the next subsection. According to the definition of the flux factor in the polar coordinate system, the flux factor is

$\mathcal{F} \equiv v_{pd} \times (|\phi_i(\mathbf{x})|^2 |\mathbf{x}|^2 d\Omega / |\mathbf{x}|^2 d\Omega) = v_{pd}$ at $|\mathbf{x}| \rightarrow \infty$ where the plane wave component $e^{i\mathbf{k}\cdot\mathbf{x}}$ dominates.

Wave Functions – In order to calculate the differential cross section Eq. (7) and later the DM production rate, one needs to specify the initial- and final-state wave functions ϕ_i and ϕ_f . The potential of the p - d system contains three parts [73],

$$V(\mathbf{x}) = V_0(x) + V_S(x)(\mathbf{l} \cdot \mathbf{s}_p) + V_C(x), \quad (8)$$

where $\mathbf{x} \equiv \mathbf{x}_p - \mathbf{x}_d$ is the relative distance between proton (\mathbf{x}_p) and deuteron (\mathbf{x}_d) with $x \equiv |\mathbf{x}|$. The nuclear and spin-orbital interactions $V_0(x)$ and $V_S(x)$ are parametrized as

$$V_0(x) = V_0 f_0(x), \quad V_S(x) = -V_S \frac{1}{m_\pi^2} \frac{1}{x} \frac{df_S(x)}{dx}, \quad (9)$$

using the Woods-Saxon potential with pion mass m_π and [80]

$$f_{0,S}(r) = \left[1 + \exp\left(\frac{r - R_{0,S}}{a_{0,S}}\right) \right]^{-1}. \quad (10)$$

For the process of p - d fusion, the parameterization constants are [75],

$$V_0 = -44.43 \text{ MeV}, \quad R_0 = R_S = 1.803 \text{ fm}, \quad (11a)$$

$$V_S = -10 \text{ MeV}, \quad a_0 = a_S = 0.65 \text{ fm}. \quad (11b)$$

The spin-orbital term contains the orbital angular momentum operator \mathbf{l} and the proton spin operator \mathbf{s}_p . Finally, $V_C(x)$ is the Coulomb potential,

$$V_C(x) = \begin{cases} \frac{Z_p Z_{de} e^2}{x} & x > R_C, \\ \frac{Z_p Z_{de} e^2}{2R_C} \left(3 - \frac{x^2}{R_C^2}\right) & x < R_C. \end{cases} \quad (12)$$

Here, $Z_{p(d)} = 1$ denotes the charge number of p (d) and $R_C = 1.803$ fm is the charge radius [75].

Since the typical energies are $\mathcal{O}(\text{MeV})$ at most, the initial ionized state wave function $\phi_i(\mathbf{x})$ and its final bound state counterpart $\phi_f(\mathbf{x})$ of the p - d system are solved with the non-relativistic Schrödinger equation. Owing to the spherical symmetry of the interacting potential Eq. (8), the wave function of any state can be decomposed into a radial and an angular component as,

$$\Psi_{EJM}(\mathbf{x}) \equiv \frac{u_{lj}^J(E, x)}{x} \mathcal{Y}_{JM}^{lj}. \quad (13)$$

where E is the energy eigenvalue of the state. Since the p - d system contains two spin information (s_p, m_{s_p}) and (s_d, m_{s_d}) for the proton and deuteron, respectively, we choose to first couple the orbital angular momentum wave function Y_{l,m_l} with the proton spin wave function $|s_p m_{s_p}\rangle$ to give $|jm_j\rangle \equiv \sum_{m_l, m_{s_p}} \langle l m_l s_p m_{s_p} | jm_j \rangle Y_{l,m_l} |s_p m_{s_p}\rangle$. Then $|jm_j\rangle$ further couples with the deuteron spin wave function $|s_d m_{s_d}\rangle$ to give the angular wave function,

$$\mathcal{Y}_{JM}^{lj} \equiv \sum_{m_j, m_{s_d}} \langle jm_j s_d m_{s_d} | JM \rangle |jm_j\rangle |s_d m_{s_d}\rangle. \quad (14)$$

Note that the proton is spin half ($s_p = 1/2$) while deuteron has spin one ($s_d = 1$). The factors labeled as $\langle \cdot | \cdot \rangle$ denotes the Clebsch–Gordan coefficients.

The radial wave function u_{lj}^J is the solution of the radial Schrödinger equation,

$$\left[-\frac{\hbar^2}{2\mu_{pd}} \left(\frac{d^2}{dx^2} - \frac{l(l+1)}{x^2} \right) + V(x) \right] u_{lj}^J = E u_{lj}^J, \quad (15)$$

where the inner product of angular momenta in Eq. (8) is 1. $s_p \equiv [j(j+1) - l(l+1) - s_p(s_p+1)]/2$ and the reduced mass is $\mu_{pd} \equiv m_p m_d / (m_p + m_d)$.

The initial ionized state with center-of-mass energy E can be described by a superposition of the eigen-wavefunctions in Eq. (13) with different angular momenta. We can define a parameter called the asymptotic momentum $k \equiv \sqrt{2\mu_{pd}E}$ and label such a state as,

$$|i\rangle \equiv \sum_{ljJM} C_{ljJM}^{km_{s_p}m_{s_d}} |k, [(ls_p)js_d]JM\rangle. \quad (16)$$

Here, the structure of the brackets represents the order of angular momentum coupling. The quantum numbers l and s_p within the parentheses are first coupled to form j in the square brackets, which further couples with s_d to yield the total angular momentum J . Along the incident direction, the plane wave is expanded as $e^{i\mathbf{k}||\mathbf{r}|\cos\theta} \equiv \sum_l (2l+1) i^l j_l(|\mathbf{k}||\mathbf{r}|) P_l(\cos\theta)$ without dependence on the azimuthal angle. Since the Legendre function P_l is proportional to the spherical harmonic function Y_l^0 with magnetic quantum number $m = 0$, the expansion coefficients are,

$$C_{ljJM}^{km_{s_p}m_{s_d}} \equiv \frac{\sqrt{(4\pi)(2l+1)}}{k} i^l \times \langle jm_{s_p} | l0 s_p m_{s_p} \rangle \langle JM | jm_{s_p} s_d m_{s_d} \rangle. \quad (17)$$

Both the nuclear and spin-orbital interactions V_0 and V_S are short-range, if we consider the region that x is large enough, only the Coulomb potential survives. Therefore, the initial ionized radial wave function $u_{lj}^J(k, x \rightarrow \infty)$ has a general form of solution as,

$$u_{lj}^J = \frac{i}{2} \left[H_l^{(-)}(\eta, kx) - S_l H_l^{(+)}(\eta, kx) \right] e^{i\sigma_l} \quad (18)$$

with $H_l^{(\pm)}$ being the spherical Coulomb functions [81]. Here, the parameters are defined as $\eta \equiv Z_p Z_d \mu_{pd} / 4\pi k$ and $\sigma_l \equiv \arg \Gamma(1+l)$. The influence of short-range interactions shows up in the factor $S_l \equiv e^{2i\delta_l}$ where δ_l is the corresponding phase shift and can be determined by matching Eq. (18) with the Schrödinger equation solution Eq. (15) at small radius. The wave function Eq. (18) is valid only at larger radii (e.g., $x > x_0$ where $x_0 \gtrsim 10^{-15} \text{ m}$). For $x < x_0$, the wave function u_s must be obtained by numerically solving the Schrödinger equation with the boundary condition $u_s(x=0) = 0$ [82] and an unknown derivative condition $u_s'(x=0) = y$. At $x = x_0$, the continuity condition requires that the two wave functions match

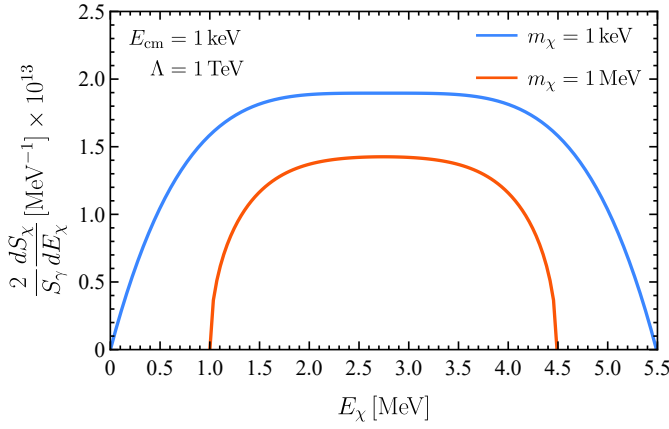


FIG. 2. The ratio of the DM and photon production S -factors for the p - d fusion.

both in value and in their first derivatives. This allows determination of the derivative y and the phase shift δ_l .

The final state is the ground state of the bound p - d system with energy level $n = 0$, since ${}^3\text{He}$ has no other excited states [83]. It also has the fixed ground-state angular quantum numbers as, $l = 0$, $j = \frac{1}{2}$, and $J = \frac{1}{2}$. As a result, the final state is simply,

$$|f\rangle = \left| n = 0, \left[\left(0 \frac{1}{2} \right) \frac{1}{2} 1 \right] \frac{1}{2} M' \right\rangle, \quad (19)$$

where M' denotes the spin direction of the ${}^3\text{He}$ state. For a bound state, the short-range interactions in Eq. (9) cannot be neglected. Consequently, the corresponding radial wave function must resort to numerical solutions and it should satisfy the boundary conditions that $u_{ij}^J(x = 0) = u_{ij}^J(x = \infty) = 0$.

By employing both the ionized and bound state wave functions, one can compute the inner product appearing in the differential cross section Eq. (7) and subsequently derive the DM production rate inside the Sun.

Production Rate – Since the deuteron number density is not publicly available in the B16-GS98 solar model [68], it is more convenient to deduce the DM production rate from the photon production processes in the p - d fusion. With exactly the same initial states, their production rates in a volume element dV_\odot are proportional to their cross sections (σ_γ for photon and σ_χ for DM),

$$\frac{d^3 N_\chi}{dtdE_\chi dV_\odot} = 2 \frac{1}{\langle \sigma_\gamma v_{\text{rel}}^{pd} \rangle} \left\langle \frac{d\sigma_\chi}{dE_\chi} v_{\text{rel}}^{pd} \right\rangle \frac{d^2 N_\gamma}{dtdV_\odot}, \quad (20)$$

where $\langle \dots \rangle$ stands for thermal average [84] of the corresponding cross section times the relative velocity v_{rel}^{pd} . The prefactor 2 accounts for the two DM particles produced in one fusion. Although the photon production rate $d^2 N_\gamma / dtdV_\odot$ is not directly provided in the Solar Model either, its value equals the sum of the pp and pep neutrino production rates [68]. Thus, the DM production rate is

linearly related to this sum throughout the Sun. Given that the pp and pep neutrino are primarily produced in the central region, DM is also predominantly produced in the solar core.

For small total kinetic energy E_{cm} of the initial-state nuclei, the fusion is exponentially suppressed, since the incoming nuclei have to penetrate the Coulomb barrier [85]. We define the S -factor to accommodate the exponential dependence [85], $S_{\chi,\gamma}(E_{\text{cm}}) \equiv \sigma_{\chi,\gamma}(E_{\text{cm}}) E_{\text{cm}} e^{2\pi\eta}$ where $\eta \equiv Z_p Z_d \mu / (4\pi \hbar^2 k)$ is a function of the proton and deuteron charge numbers $Z_{p,d}$, the reduced mass $\mu \equiv m_p m_d / (m_p + m_d)$, and the center-of-mass momentum $k = \sqrt{2\mu E_{\text{cm}}}$. Different from cross section, the S -factor tends to be a constant at low energy, $S_{\chi,\gamma}(E_{\text{cm}}) \simeq S_{\chi,\gamma}$ [85]. Since $E_{\text{cm}} e^{2\pi\eta}$ is independent of E_χ , the cross sections $\sigma_{\chi,\gamma}$ in Eq. (20) can be replaced by the S factors,

$$\frac{d^3 N_\chi}{dtdE_\chi dV_\odot} \simeq \frac{2}{S_\gamma} \frac{dS_\chi}{dE_\chi} \frac{d^2 N_\gamma}{dtdV_\odot}. \quad (21)$$

The ratio of production rates is proportional to the ratio of S -factors. Fig. 2 shows that the DM production rate with $\Lambda = 1 \text{ TeV}$ is nearly 13 orders of magnitude smaller than its photon counterpart. Although the cooling effect due to DM release is negligible, the produced DM flux can be probed at the DM direct detection experiments.

III. Solar Attenuation with Three-Dimensional Analytic Boltzmann Equation Formalism

When propagating inside the Sun, the DM particle scatters with nuclei (mainly protons and α particles) and roams until reaching the solar surface. These scatterings would attenuate and soften the DM flux. Although the DM attenuation can be addressed with both analytic [31, 38, 41, 86, 87] and Monte Carlo [43, 56, 88–91] methods, they have their own limitations. Especially, the existing analytic methods based on the ballistic approximation assume that DM propagates in straight lines which is not appropriate for multiple scatterings with large scattering angle. For the convolutional approach that sums up all the DM fluxes after multiple scattering [92], it currently only applies to a homogeneous slab-shaped medium with isotropic scattering.

We propose using the Boltzmann method to precisely and efficiently calculate the solar attenuation effect. The Boltzmann equation describes the evolution of the distribution function $f_\chi(\mathbf{r}_\chi, \mathbf{p}_\chi, t)$,

$$\hat{\mathbf{L}}[f_\chi] = \mathbf{C}_{xp}[f_\chi] + \mathbf{C}_{x\alpha}[f_\chi] + \mathbf{C}_{\text{prod}}, \quad (22)$$

where $\hat{\mathbf{L}}[f_\chi]$ is the Liouville operator [84, 93] and \mathbf{Cs} are collision terms [84, 94]. Due to the spherical symmetry of the Sun, the distribution function $f_\chi(\mathbf{r}_\chi, \mathbf{p}_\chi, t)$ is independent of the solid angles of \mathbf{r}_χ and depends only on the radial coordinate $r \equiv |\mathbf{r}_\chi|$. At any given location \mathbf{r}_χ , the momentum distribution of DM remains rotationally symmetric about the axis along \mathbf{r}_χ . Thus, $f_\chi(\mathbf{r}_\chi, \mathbf{p}_\chi, t)$

is also independent of the azimuthal angle of \mathbf{p}_χ . Assuming the Sun has reached steady state, we can further neglect the time dependence in $f_\chi(\mathbf{r}_\chi, \mathbf{p}_\chi, t)$. As a result, $f_\chi(\mathbf{r}_\chi, \mathbf{p}_\chi, t)$ depends only on three variables: the radial distance r , the angle between the position vector and the momentum (or its cosine u), and the magnitude of the momentum (or energy E_χ), $f_\chi(\mathbf{r}_\chi, \mathbf{p}_\chi, t) \rightarrow f_\chi(r, u, E_\chi)$.

Of the collision terms [84, 94], the first two $\mathbf{C}_{\chi p}[f_\chi]$ and $\mathbf{C}_{\chi\alpha}[f_\chi]$ on the right-hand side describe the elastic scattering of DM with a proton or alpha particle target, respectively. Each contains two contributions, $\mathbf{C}_{\chi p}[f_\chi] \equiv \mathbf{C}_{\chi p}^{(1)}[f_\chi] + \mathbf{C}_{\chi p}^{(2)}[f_\chi]$ and $\mathbf{C}_{\chi\alpha}[f_\chi] \equiv \mathbf{C}_{\chi\alpha}^{(1)}[f_\chi] + \mathbf{C}_{\chi\alpha}^{(2)}[f_\chi]$, for flowing out or into the phase space point under consideration [38].

The first χ - p scattering collision term, $\mathbf{C}_{\chi p}^{(1)}[f_\chi]$, describes an outflux of DM with kinematic variables (u, E_χ) ,

$$\mathbf{C}_{\chi p}^{(1)}[f_\chi] \equiv -E_\chi f_\chi \int \frac{g_p d^3 \mathbf{p}_p}{(2\pi)^3} f_p(|\mathbf{p}_p|) \sigma_{\chi p} v_{\text{rel}}^{\chi p}, \quad (23)$$

with $g_p = 2$ counting the proton spin. The integral above is a thermal average of the χ - p scattering cross section $\sigma_{\chi p}$ times the relative velocity $v_{\text{rel}}^{\chi p}$ over the proton Boltzmann distribution $f_p(|\mathbf{p}_p|)$. For comparison, the second term $\mathbf{C}_{\chi p}^{(2)}[f_\chi]$ describes a DM influx from the kinematic variables (u', E'_χ) ,

$$\mathbf{C}_{\chi p}^{(2)}[f_\chi] \equiv \int d\Pi_{p'} f_p(|\mathbf{p}'_p|) \int \frac{d\Omega'_\chi}{8(2\pi)^2} f_\chi(r, u', E'_\chi) A \quad (24)$$

with

$$A \equiv \frac{|\mathbf{p}'|^2 |\mathcal{M}_{\chi p}|^2}{|\mathbf{p}'_\chi|(E_\chi - E_p) - |\mathbf{p}_\chi - \mathbf{p}'_p| E'_\chi \cos \tilde{\theta}}, \quad (25)$$

$d\Pi_{p'} \equiv \frac{g_p d^3 \mathbf{p}'_p}{(2\pi)^3 2E_p}$, and $|\mathcal{M}_{\chi p}|^2 = 4m_p^2/\Lambda^2$ being the spin-averaged squared χ - p scattering amplitude. The solid angle Ω'_χ is for the incoming DM particle while $\tilde{\theta}$ is the angle between the initial-state DM momentum \mathbf{p}'_χ and the difference $(\mathbf{p}_\chi - \mathbf{p}'_p)$ between the final DM (\mathbf{p}_χ) and the initial proton (\mathbf{p}'_p) momenta. Note that the incoming DM energy E'_χ is not an independent variable here but is determined by the energy-momentum conservation.

The two integration terms Eq. (23) and Eq. (24) are complicated. Since the proton mass (\simeq GeV) is much larger than the proton and DM momentum as well as the DM energy (\sim MeV), the two collision terms can be expanded up to $\mathcal{O}(1/m_p)$ for convenience. The expansion of $\sigma_{\chi p} v_{\text{rel}}^{\chi p}$ gives,

$$\sigma_{\chi p} v_{\text{rel}}^{\chi p} \simeq \sigma_{\chi p}^{\text{LO}} v_\chi \left(1 - \frac{2E_\chi}{m_p} - \frac{E_\chi |\mathbf{p}_p|}{m_p |\mathbf{p}_\chi|} \cos \theta_{\chi p} \right), \quad (26)$$

where $\sigma_{\chi p}^{\text{LO}} \equiv 1/4\pi\Lambda^2$ is the leading-order contribution to the χ - p scattering cross section. The term proportional to $\cos \theta_{\chi p}$ vanishes after integrating over the solid angles of \mathbf{p}_p . The first collision term then becomes,

$$\mathbf{C}_{\chi p}^{(1)}[f_\chi] \simeq -|\mathbf{p}_\chi| n_p \sigma_{\chi p}^{\text{LO}} f_\chi(r, u, E_\chi) \left(1 - \frac{2E_\chi}{m_p} \right), \quad (27)$$

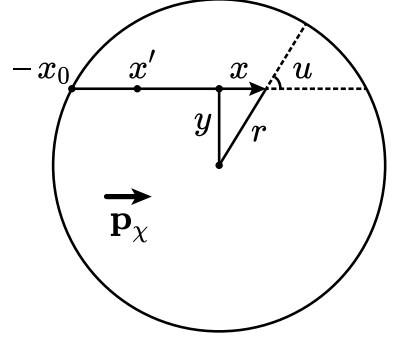


FIG. 3. Illustration of the geometric meaning of x and y . x' denotes the integration variable in the integral equation form of the Boltzmann equation. $-x_0$ is on the solar surface.

where n_p is the proton number density.

In contrast, the expansion of Eq. (24) is more intricate due to the dependence of $f_\chi(r, u', E'_\chi)$ on the variable E'_χ , which is a function of integration variables and should also be expanded. To address this, we perform a Taylor expansion of the unknown function $f_\chi(r, u', E'_\chi)$ around $E'_\chi = E_\chi$,

$$f_\chi \approx f_\chi(r, u', E_\chi) + \frac{\partial f_\chi(r, u', E_\chi)}{\partial E_\chi} (E'_\chi - E_\chi). \quad (28)$$

This allows extraction of E'_χ from the function f_χ , enabling further expansion in $\mathcal{O}(1/m_p)$ and subsequent integration as well as simplification. Since $f_\chi(r, u', E_\chi)$ in both terms depends only on u' but no longer E'_χ , the integrations over $d\Pi_{p'}$ and the azimuthal angle $d\phi'$ of Ω'_χ only applies to E'_χ . Defining an averaged \bar{E}'_χ ,

$$\bar{E}'_\chi \equiv \frac{\int d\phi' d\Pi_{p'} f_p(|\mathbf{p}'_p|) A E'_\chi}{\int d\phi' d\Pi_{p'} f_p(|\mathbf{p}'_p|) A}, \quad (29)$$

one can factor out the term $\int d\phi' d\Pi_{p'} f_p(|\mathbf{p}'_p|) A$ from the integral in Eq. (24) and simply replace E'_χ in Eq. (28) with \bar{E}'_χ . Then, inserting Eq. (28) yields an integral expression for the function $f_\chi(r, u', \bar{E}'_\chi)$,

$$\mathbf{C}_{\chi p}^{(2)}[f_\chi] \simeq \int \frac{du'}{32\pi^2} f_\chi(r, u', \bar{E}'_\chi) \int d\phi' d\Pi_{p'} f_p(|\mathbf{p}'_p|) A, \quad (30)$$

The factor A defined in Eq. (24) can be expanded up to $\mathcal{O}(1/m_p)$ as

$$A \simeq \frac{|\mathbf{p}_\chi| |\mathcal{M}_{\chi p}|^2}{m_p} \left[1 + \frac{2E_\chi}{m_p} (1 - \cos \theta_{\chi\chi'}) + \dots \right], \quad (31)$$

where $\theta_{\chi\chi'}$ denotes the opening angle between the initial- and final-state DM particles. The omitted terms ... in Eq. (31) contains $\cos \theta_{\chi'p'}$ and $\cos \theta_{\chi p'}$, which vanish after integration over the solid angle of \mathbf{p}'_p . Besides, the integration of $\cos \theta_{\chi\chi'} = uu' + \sqrt{1-u^2}\sqrt{1-u'^2} \cos \phi'$

over $d\phi'$ yields $2\pi uu'$ to give,

$$\int d\phi' d\Pi_{p'} f_p A \simeq 16\pi^2 |\mathbf{p}_\chi| n_p \sigma_{\chi p}^{\text{LO}} \left[1 + \frac{2E_\chi}{m_p} (1 - uu') \right]. \quad (32)$$

Similarly, the factor \bar{E}'_χ in Eq. (29) can be expanded up to $\mathcal{O}(1/m_p)$. Using the expansion of E'_χ ,

$$E'_\chi = E_\chi + \frac{|\mathbf{p}_\chi|^2}{m_p} (1 - \cos \theta_{\chi\chi'}) + \dots, \quad (33)$$

the integration in Eq. (29) can be evaluated in the same manner as in Eq. (32), giving

$$\bar{E}'_\chi \simeq E_\chi + \frac{|\mathbf{p}_\chi|^2}{m_p} (1 - uu'). \quad (34)$$

Putting things together, the final expansion of Eq. (24) is given by

$$\begin{aligned} \mathbf{C}_{\chi p}^{(2)}[f_\chi] &\simeq |\mathbf{p}_\chi| n_p \sigma_{\chi p}^{\text{LO}} \int \frac{du'}{2} f_\chi(r, u', \bar{E}'_\chi) \\ &\quad \times \left[1 + \frac{2E_\chi}{m_p} (1 - uu') \right]. \end{aligned} \quad (35)$$

The integrals are now greatly simplified.

Similar simplification can also apply to the $\chi\text{-}\alpha$ collision terms, $\mathbf{C}_{\chi\alpha}^{(1,2)}[f_\chi]$. Note that the $\chi\text{-}\alpha$ scattering cross section $\sigma_{\chi\alpha}^{\text{LO}} = Z_\alpha^2 \sigma_{\chi p}^{\text{LO}}$ is coherently enhanced by the ${}^4\text{He}$ charge $Z_\alpha = 2$.

The remaining $\mathbf{C}_{\text{prod}} \equiv \frac{2\pi^2}{|\mathbf{p}_\chi|} \frac{d^3 N_\chi}{dt dE_\chi dV_\odot}$ is actually a source term from the DM production that also happens all over the Sun as given in Eq. (21).

To uniquely solve the differential Boltzmann equation in Eq. (22), we need a boundary condition that no DM particle enters the solar surface, $f_\chi(R_\odot, u, E_\chi) = 0$ for $u \leq 0$, where R_\odot is the solar radius. In the spherical coordinate system, the Liouville operator appearing on the left-hand side of Eq. (22) can be expressed as,

$$\hat{\mathbf{L}}[f_\chi] = |\mathbf{p}_\chi| \left(u \frac{\partial f_\chi}{\partial r} + \frac{1 - u^2}{r} \frac{\partial f_\chi}{\partial u} \right). \quad (36)$$

By making the variable substitution $x \equiv ru$ and $y \equiv r\sqrt{1 - u^2}$, the Liouville operator reduces to a single derivative, $\hat{\mathbf{L}}[f_\chi] = |\mathbf{p}_\chi| \partial_x f_\chi$. The variable x denotes the DM position along its propagation line, and together with y , they form a Cartesian coordinate system (see in Fig. 3). The solution to the Boltzmann equation Eq. (22) is then an integral equation with the integration constant fixed by the boundary condition,

$$\begin{aligned} f_\chi(r, u, E_\chi) &= \int_{-x_0}^x dx' e^{-\int_{x'}^x \sum_i n_i(r(x'', y)) \sigma'_{\chi i} dx''} \left[\frac{2\pi^2}{|\mathbf{p}_\chi|^2} \frac{d^3 N_\chi}{dt dE_\chi dV_\odot}(r(x', y), E_\chi) \right] \\ &\quad + \int_{-x_0}^x dx' e^{-\int_{x'}^x \sum_i n_i(r(x'', y)) \sigma'_{\chi i} dx''} \sum_i n_i(r(x', y)) \sigma_{\chi i}^{\text{LO}} \int \frac{du'}{2} f_\chi(r(x', y), u', \bar{E}'_i) \left[1 + \frac{2E_\chi(1 - uu')}{m_i} \right], \end{aligned} \quad (37)$$

where $i = (p, \alpha)$ labels the scattering targets. In addition, $\sigma'_{\chi i} \equiv \sigma_{\chi i}^{\text{LO}} (1 - 2E_\chi/m_i)$ and $\bar{E}'_i \equiv E_\chi + |\mathbf{p}_\chi|^2 (1 - uu')/m_i$. The radial function is defined as $r(x, y) \equiv \sqrt{x^2 + y^2}$ and $x_0 \equiv \sqrt{R_\odot^2 - y^2}$ corresponds to the solar surface.

This integral equation has clear physical interpretation. The first term on the right-hand side represents the contribution to $f_\chi(r, u, E_\chi)$ from the DM production at position (x', y) that propagates from x' to x without scattering. The exponential factor corresponds to the probability of propagation without scattering. The second term accounts for the contribution to $f_\chi(r, u, E_\chi)$ from those DM particles, originally characterized by the kinematic variables (u', \bar{E}'_i) , that scatter at position (x', y) into (u, E_χ) and then propagate from x' to x without further scattering.

When propagating from the solar surface to our Earth, the DM flux

$$\frac{d\Phi_\oplus}{dE_\chi} = \frac{R_\odot^2}{\text{AU}^2} |\mathbf{p}_\chi|^2 \int_0^1 \frac{du}{4\pi^2} u f(R_\odot, u, E_\chi), \quad (38)$$

is diluted by a factor of R_\odot^2/AU^2 where AU is the astronomical unit. Fig. 4 shows the DM flux spectrum at the Earth for $m_\chi = 1 \text{ MeV}$ and $\sigma_{\chi p}^{\text{LO}} = 10^{-34} \text{ cm}^2$. Our result (red thin line) is verified by the Monte Carlo simulation with `DarkProp` [95]. The solar attenuation effect can significantly change the DM spectrum. The quite flat spectrum in the middle as shown by Fig. 2 is attenuated to a low energy peak in Fig. 4.

We note that there is a boundary in scattering cross section between severe and mild attenuation. It can be estimated using the number of scatterings of DM across the sun, $\int_0^{R_\odot} (n_p \sigma_{\chi p}^{\text{LO}} + n_\alpha \sigma_{\chi\alpha}^{\text{LO}}) dr \sim 30$. We choose the number of scatterings to be 30 typically instead of 1 because DM loses only $\sim 10^{-3}$ of its energy in each scattering and it can scatter several times before escaping without losing too much energy. From this we can derive the typical boundary as $\sigma_{\chi p}^{\text{LO}} \sim 4 \times 10^{-35} \text{ cm}^2$. For smaller scattering cross section, the attenuation effects can be neglected.

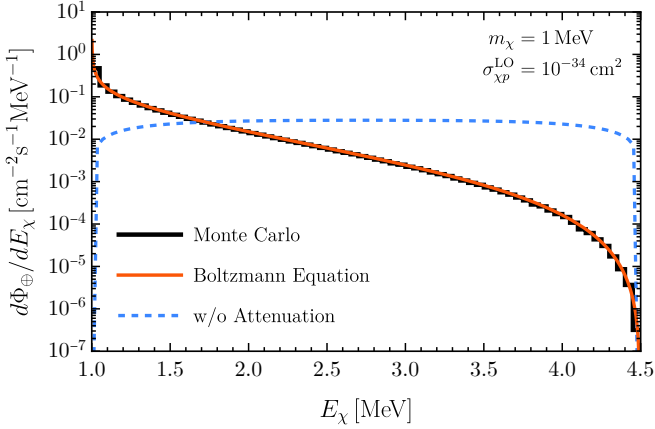


FIG. 4. The solar DM flux spectrum arriving at Earth for $m_\chi = 1$ MeV and $\sigma_{\chi p}^{\text{LO}} = 10^{-34} \text{ cm}^2$. The red curve is from the analytic Boltzmann equation method while the black curve is from Monte Carlo simulation based on `DarkProp` [95]. The blue dashed curve is obtained assuming no attenuation.

IV. Direct Detection of MeV Solar Dark Matter

When reaching Earth, the solar DM can be detected in direct detection experiments. For xenon-based detectors, the maximal recoil energy for a xenon nucleus with mass $m_{\text{Xe}} \simeq 2|\mathbf{p}_\chi|^2/m_{\text{Xe}} \simeq 0.4 \text{ keV}$ where $|\mathbf{p}_\chi| \simeq 5.5 \text{ MeV}$ is the maximal momentum as shown in Fig. 2, is below the Xenon1T (0.7 keV) and PandaX-4T (0.77 keV) S2-only thresholds [96, 97]. For argon-based detectors, the recoil energy can reach $T_{\text{N}}^{\text{Ar}} \simeq 1.5 \text{ keV}$ to exceed the threshold (0.6 keV, corresponding to the number of ionization electrons $N_{e^-} = 4$) of DarkSide-50 [98, 99].

In the limit of weak χ - p coupling, the solar DM production and event rate decreases accordingly. In the strong coupling limit, although the solar DM can be abundantly produced, the solar attenuation effect becomes severe and DM loses too much energy inside the Sun such that the DM event rate above threshold also decreases. Furthermore, the DM detection spectrum drops at large recoil energy as shown in Fig. 4. Thus, there is a maximum of the solar DM event rate, $\simeq 10^{-5}/N_{e^-} \cdot \text{kg} \cdot \text{day}$, at the threshold $N_{e^-} = 4$. For comparison, the background of Darkside-50 at $N_{e^-} = 4$ is around $10^{-2}/N_{e^-} \cdot \text{kg} \cdot \text{day}$ [98]. Therefore, the sensitivity of Darkside-50 is not sufficient to detect solar DM. However, the next-generation detector, DarkSide-LowMass (DS-LM) [100], with larger fiducial mass ($\simeq 1$ ton compared to $\simeq 20$ kg in DarkSide-50), lower threshold, and reduced background ($\simeq 10^{-4}/N_{e^-} \cdot \text{kg} \cdot \text{day}$ at the threshold $N_{e^-} = 2$), is capable of detecting solar DM. At DarkSide-LowMass, the major background from ^{39}Ar is projected to be $7.3 \mu\text{Bq}/\text{kg}$ or $73 \mu\text{Bq}/\text{kg}$ [100].

Assuming a $1 \text{ ton} \cdot \text{year}$ exposure, we show the projected 90% C.L. limits as colored curves in Fig. 5. The DarkSide-LowMass experiment is sensitive to the sub-MeV solar DM with a scattering cross section $10^{-35} \text{ cm}^2 \lesssim \sigma_{\chi p}^{\text{LO}} \lesssim 4 \times 10^{-34} \text{ cm}^2$, which is two orders lower than the current

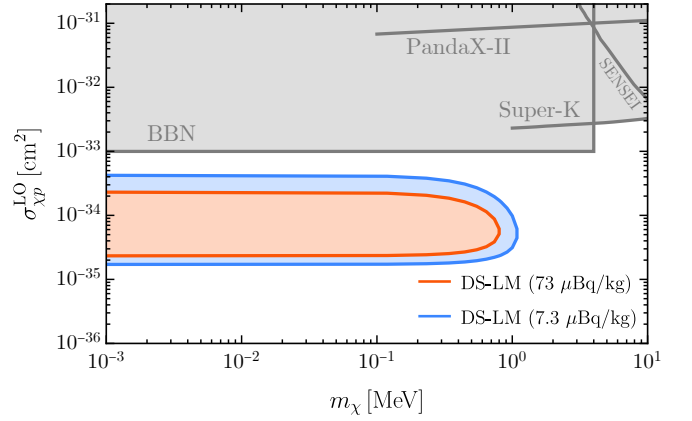


FIG. 5. The projected exclusion regions for the solar DM parameter space at DarkSide-LowMass with a ^{39}Ar background level of $73 \mu\text{Bq}/\text{kg}$ (red) or $7.3 \mu\text{Bq}/\text{kg}$ (blue). For comparison, the exclusion limits from PandaX [101] and Super-Kamiokande [102] on the cosmic-ray boosted DM, SENSEI [103], as well as the BBN constraint are also shown.

limits from the cosmic-ray boosted DM [101, 102], while the conventional direct detection can only reach 10^{-27} cm^2 at the SENSEI experiment [103]. Since the relevant DM mass range is well below the production energy, both the upper and lower boundaries are almost independent of the DM mass and can extend to very tiny mass.

Usually, sub-MeV DM is stringently constrained by the big bang nucleosynthesis (BBN) [104–109]. If thermally coupled to the SM plasma, a complex scalar DM with mass $\lesssim 4$ MeV is excluded by BBN [108]. Such constraint can be alleviated if DM decouples with SM particles first and then is diluted to a smaller density before BBN [110]. The dilution can be induced by a heavy out-of-equilibrium particle decaying into SM particles. Note that the decay process may also dilute neutrinos. To keep neutrinos unchanged, it should happen earlier than neutrino decoupling, which requires the decay width $\Gamma > 10^{-23} \text{ GeV}$ [111]. After dilution, the complex scalar DM should have a lower temperature T_χ than that of the SM plasma T_{SM} , $T_\chi < 0.77 T_{\text{SM}}$ [112], to be compatible with BBN. Equivalently, this requires that DM decouples earlier than the heavy particle decay, $H(T_{\text{dec}}) > 2.25 \Gamma$ where $H(T_{\text{dec}})$ denotes the Hubble rate at the decoupling temperature T_{dec} . Thus, the minimal decoupling temperature is $T_{\text{dec}} > 7.05 \text{ MeV}$. In our scenario, the DM decoupling is controlled by the tree level $p + \bar{p} \rightarrow \chi + \chi^*$, $\gamma + p \rightarrow p + \chi + \chi^*$ process, as well as the loop-induced $\gamma + \gamma \rightarrow \chi + \chi^*$ process. Since the proton number density is exponentially suppressed at low temperature, the latter process dominates and the aforementioned lower bound on T_{dec} then transfers to $\Lambda > 176 \text{ GeV}$. In other words, a light complex scalar DM can be compatible with BBN, if the χ - p scattering cross section is small enough, $\sigma_{\chi p}^{\text{LO}} < 9.97 \times 10^{-34} \text{ cm}^2$, as shown in Fig. 5.

V. Conclusion

Not just the thermal and atomic processes inside the Sun can evaporate DM or produce light DM such as axion, but also the nuclear fusion can produce energetic MeV DM particles. We provide a concrete example of the proton deuteron fusion process that during the p - d system transition from an ionized state to its bound state, namely the ^3He nuclei, a pair of DM particles are produced. With an energy release of 5.5 MeV, the produced DM can overcome the direct detection threshold. Being not strongly constrained, the produced solar DM can experience strong attenuation inside the Sun. With spherical symmetry, the Boltzmann equation can be used to describe the attenuation quite well.

Acknowledgements

The authors would like to thank Junting Huang and Yi Wang for useful discussions. Chuan-Yang Xing and Chen Xia are supported by the National Natural Science Foundation of China (Nos. 12247141, 12247148). Shao-Feng Ge is supported by the National Natural Science Foundation of China (Nos. 12375101, 12425506, 12090060, 12090064) and the SJTU Double First Class start-up fund (WF220442604). SFG is also an affiliate member of Kavli IPMU, University of Tokyo.

[1] Bing-Lin Young, “*A survey of dark matter and related topics in cosmology*,” *Front. Phys. (Beijing)* **12** no. 2, (2017) 121201. [Erratum: *Front.Phys.(Beijing)* 12, 121202 (2017)].

[2] Martin Bauer and Tilman Plehn, *Yet Another Introduction to Dark Matter: The Particle Physics Approach*, vol. 959 of Lecture Notes in Physics. Springer, 2019. [[arXiv:1705.01987](#) [hep-ph]].

[3] Tongyan Lin, “*Dark matter models and direct detection*,” *PoS* **333** (2019) 009, [[arXiv:1904.07915](#) [hep-ph]].

[4] A. Arbey and F. Mahmoudi, “*Dark matter and the early Universe: a review*,” *Prog. Part. Nucl. Phys.* **119** (2021) 103865, [[arXiv:2104.11488](#) [hep-ph]].

[5] Jodi Cooley, “*Dark Matter direct detection of classical WIMPs*,” *SciPost Phys. Lect. Notes* **55** (2022) 1, [[arXiv:2110.02359](#) [hep-ph]].

[6] **PandaX-4T** Collaboration, Yue Meng et al., “*Dark Matter Search Results from the PandaX-4T Commissioning Run*,” *Phys. Rev. Lett.* **127** no. 26, (2021) 261802, [[arXiv:2107.13438](#) [hep-ex]].

[7] **LZ** Collaboration, J. Aalbers et al., “*First Dark Matter Search Results from the LUX-ZEPLIN (LZ) Experiment*,” *Phys. Rev. Lett.* **131** no. 4, (2023) 041002, [[arXiv:2207.03764](#) [hep-ex]].

[8] **XENON** Collaboration, E. Aprile et al., “*First Dark Matter Search with Nuclear Recoils from the XENONnT Experiment*,” *Phys. Rev. Lett.* **131** no. 4, (2023) 041003, [[arXiv:2303.14729](#) [hep-ex]].

[9] Chris Kouvaris and Josef Pradler, “*Probing sub-GeV Dark Matter with conventional detectors*,” *Phys. Rev. Lett.* **118** no. 3, (2017) 031803, [[arXiv:1607.01789](#) [hep-ph]].

[10] Masahiro Ibe, Wakutaka Nakano, Yutaro Shoji, and Kazumine Suzuki, “*Migdal Effect in Dark Matter Direct Detection Experiments*,” *JHEP* **03** (2018) 194, [[arXiv:1707.07258](#) [hep-ph]].

[11] Matthew J. Dolan, Felix Kahlhoefer, and Christopher McCabe, “*Directly detecting sub-GeV dark matter with electrons from nuclear scattering*,” *Phys. Rev. Lett.* **121** no. 10, (2018) 101801, [[arXiv:1711.09906](#) [hep-ph]].

[12] Daniel Baxter, Yonatan Kahn, and Gordan Krnjaic, “*Electron Ionization via Dark Matter-Electron Scattering and the Migdal Effect*,” *Phys. Rev. D* **101** no. 7, (2020) 076014, [[arXiv:1908.00012](#) [hep-ph]].

[13] Rouven Essig, Josef Pradler, Mukul Sholapurkar, and Tien-Tien Yu, “*Relation between the Migdal Effect and Dark Matter-Electron Scattering in Isolated Atoms and Semiconductors*,” *Phys. Rev. Lett.* **124** no. 2, (2020) 021801, [[arXiv:1908.10881](#) [hep-ph]].

[14] Jeff A. Dror, Gilly Elor, and Robert McGehee, “*Directly Detecting Signals from Absorption of Fermionic Dark Matter*,” *Phys. Rev. Lett.* **124** no. 18, (2020) 18, [[arXiv:1905.12635](#) [hep-ph]].

[15] Jeff A. Dror, Gilly Elor, and Robert McGehee, “*Absorption of Fermionic Dark Matter by Nuclear Targets*,” *JHEP* **02** (2020) 134, [[arXiv:1908.10861](#) [hep-ph]].

[16] Jeff A. Dror, Gilly Elor, Robert McGehee, and Tien-Tien Yu, “*Absorption of sub-MeV fermionic dark matter by electron targets*,” *Phys. Rev. D* **103** no. 3, (2021) 035001, [[arXiv:2011.01940](#) [hep-ph]]. [Erratum: *Phys. Rev. D* 105, 119903 (2022)].

[17] Shao-Feng Ge, Xiao-Gang He, Xiao-Dong Ma, and Jie Sheng, “*Revisiting the fermionic dark matter absorption on electron target*,” *JHEP* **05** (2022) 191, [[arXiv:2201.11497](#) [hep-ph]].

[18] Tong Li, Jiajun Liao, and Rui-Jia Zhang, “*Dark magnetic dipole property in fermionic absorption by nucleus and electrons*,” *JHEP* **05** (2022) 071, [[arXiv:2201.11905](#) [hep-ph]].

[19] Shao-Feng Ge and Oleg Titov, “*Incoherent Fermionic Dark Matter Absorption with Nucleon Fermi Motion*,” [[arXiv:2405.05728](#) [hep-ph]].

[20] Yohei Ema, Robert McGehee, Maxim Pospelov, and Anupam Ray, “*Dark Matter Catalyzed Baryon Destruction*,” [[arXiv:2405.18472](#) [hep-ph]].

[21] Shao-Feng Ge and Xiao-Dong Ma, “*Nucleon Consumption and Mass-Energy Conversion Induced by Dark Matter*,” [[arXiv:2406.00445](#) [hep-ph]].

[22] Yonit Hochberg, Yue Zhao, and Kathryn M. Zurek, “*Superconducting Detectors for Superlight Dark Matter*,” *Phys. Rev. Lett.* **116** no. 1, (2016) 011301, [[arXiv:1504.07237](#) [hep-ph]].

[23] Katelin Schutz and Kathryn M. Zurek, “*Detectability of Light Dark Matter with Superfluid Helium*,” *Phys. Rev. Lett.* **117** no. 12, (2016) 121302, [[arXiv:1604.08206](#) [hep-ph]].

[24] Yonit Hochberg, Ilya Charaev, Sae-Woo Nam, Varun Verma, Marco Colangelo, and Karl K. Berggren, “*Detecting Sub-GeV Dark Matter with Superconducting Nanowires*,” *Phys. Rev. Lett.* **123** no. 15, (2019) 151802, [[arXiv:1903.05101](#) [hep-ph]].

[25] Andrea Caputo, Angelo Esposito, Fulvio Piccinini, Antonio D. Polosa, and Giuseppe Rossi, “*Directional detection of light dark matter from three-phonon events in superfluid ^4He* ,” *Phys. Rev. D* **103** no. 5, (2021) 055017, [[arXiv:2012.01432](https://arxiv.org/abs/2012.01432) [hep-ph]].

[26] Angelo Esposito and Shashin Pavaskar, “*Optimal antiferromagnets for light dark matter detection*,” *Phys. Rev. D* **108** no. 1, (2023) L011901, [[arXiv:2210.13516](https://arxiv.org/abs/2210.13516) [hep-ph]].

[27] Joshua Berger, Yanou Cui, and Yue Zhao, “*Detecting Boosted Dark Matter from the Sun with Large Volume Neutrino Detectors*,” *JCAP* **02** (2015) 005, [[arXiv:1410.2246](https://arxiv.org/abs/1410.2246) [hep-ph]].

[28] Takashi Toma, “*Distinctive signals of boosted dark matter from its semiannihilation*,” *Phys. Rev. D* **105** no. 4, (2022) 043007, [[arXiv:2109.05911](https://arxiv.org/abs/2109.05911) [hep-ph]].

[29] Wen Yin, “*Highly-boosted dark matter and cutoff for cosmic-ray neutrinos through neutrino portal*,” *EPJ Web Conf.* **208** (2019) 04003, [[arXiv:1809.08610](https://arxiv.org/abs/1809.08610) [hep-ph]].

[30] Christopher V. Cappiello, Kenny C. Y. Ng, and John F. Beacom, “*Reverse Direct Detection: Cosmic Ray Scattering With Light Dark Matter*,” *Phys. Rev. D* **99** no. 6, (2019) 063004, [[arXiv:1810.07705](https://arxiv.org/abs/1810.07705) [hep-ph]].

[31] Torsten Bringmann and Maxim Pospelov, “*Novel direct detection constraints on light dark matter*,” *Phys. Rev. Lett.* **122** no. 17, (2019) 171801, [[arXiv:1810.10543](https://arxiv.org/abs/1810.10543) [hep-ph]].

[32] Yohei Ema, Filippo Sala, and Ryosuke Sato, “*Light Dark Matter at Neutrino Experiments*,” *Phys. Rev. Lett.* **122** no. 18, (2019) 181802, [[arXiv:1811.00520](https://arxiv.org/abs/1811.00520) [hep-ph]].

[33] Christopher V. Cappiello and John F. Beacom, “*Strong New Limits on Light Dark Matter from Neutrino Experiments*,” *Phys. Rev. D* **100** no. 10, (2019) 103011, [[arXiv:1906.11283](https://arxiv.org/abs/1906.11283) [hep-ph]]. [Erratum: *Phys. Rev. D* 104, 069901 (2021)].

[34] James B. Dent, Bhaskar Dutta, Jayden L. Newstead, and Ian M. Shoemaker, “*Bounds on Cosmic Ray-Boosted Dark Matter in Simplified Models and its Corresponding Neutrino-Floor*,” *Phys. Rev. D* **101** no. 11, (2020) 116007, [[arXiv:1907.03782](https://arxiv.org/abs/1907.03782) [hep-ph]].

[35] Kyrylo Bondarenko, Alexey Boyarsky, Torsten Bringmann, Marco Hufnagel, Kai Schmidt-Hoberg, and Anastasia Sokolenko, “*Direct detection and complementary constraints for sub-GeV dark matter*,” *JHEP* **03** (2020) 118, [[arXiv:1909.08632](https://arxiv.org/abs/1909.08632) [hep-ph]].

[36] Wenyu Wang, Lei Wu, Jin Min Yang, Hang Zhou, and Bin Zhu, “*Cosmic ray boosted sub-GeV gravitationally interacting dark matter in direct detection*,” *JHEP* **12** (2020) 072, [[arXiv:1912.09904](https://arxiv.org/abs/1912.09904) [hep-ph]]. [Erratum: *JHEP* 02, 052 (2021)].

[37] Gang Guo, Yue-Lin Sming Tsai, and Meng-Ru Wu, “*Probing cosmic-ray accelerated light dark matter with IceCube*,” *JCAP* **10** (2020) 049, [[arXiv:2004.03161](https://arxiv.org/abs/2004.03161) [astro-ph.HE]].

[38] Shao-Feng Ge, Jianglai Liu, Qiang Yuan, and Ning Zhou, “*Diurnal Effect of Sub-GeV Dark Matter Boosted by Cosmic Rays*,” *Phys. Rev. Lett.* **126** no. 9, (2021) 091804, [[arXiv:2005.09480](https://arxiv.org/abs/2005.09480) [hep-ph]].

[39] Qing-Hong Cao, Ran Ding, and Qian-Fei Xiang, “*Searching for sub-MeV boosted dark matter from xenon electron direct detection*,” *Chin. Phys. C* **45** no. 4, (2021) 045002, [[arXiv:2006.12767](https://arxiv.org/abs/2006.12767) [hep-ph]].

[40] Zhan-Hong Lei, Jian Tang, and Bing-Long Zhang, “*Constraints on cosmic-ray boosted dark matter in CDEX-10 **,” *Chin. Phys. C* **46** no. 8, (2022) 085103, [[arXiv:2008.07116](https://arxiv.org/abs/2008.07116) [hep-ph]].

[41] Chen Xia, Yan-Hao Xu, and Yu-Feng Zhou, “*Constraining light dark matter upscattered by ultrahigh-energy cosmic rays*,” *Nucl. Phys. B* **969** (2021) 115470, [[arXiv:2009.00353](https://arxiv.org/abs/2009.00353) [hep-ph]].

[42] Jie-Cheng Feng, Xian-Wei Kang, Chih-Ting Lu, Yue-Lin Sming Tsai, and Feng-Shou Zhang, “*Revising inelastic dark matter direct detection by including the cosmic ray acceleration*,” *JHEP* **04** (2022) 080, [[arXiv:2110.08863](https://arxiv.org/abs/2110.08863) [hep-ph]].

[43] Chen Xia, Yan-Hao Xu, and Yu-Feng Zhou, “*Production and attenuation of cosmic-ray boosted dark matter*,” *JCAP* **02** no. 02, (2022) 028, [[arXiv:2111.05559](https://arxiv.org/abs/2111.05559) [hep-ph]].

[44] Chen Xia, Yan-Hao Xu, and Yu-Feng Zhou, “*Azimuthal asymmetry in cosmic-ray boosted dark matter flux*,” *Phys. Rev. D* **107** no. 5, (2023) 055012, [[arXiv:2206.11454](https://arxiv.org/abs/2206.11454) [hep-ph]].

[45] Wenyu Wang, Wu-Long Xu, Jin Min Yang, and Rui Zhu, “*Direct detection of cosmic ray-boosted puffy dark matter*,” *Nucl. Phys. B* **995** (2023) 116348, [[arXiv:2305.12668](https://arxiv.org/abs/2305.12668) [hep-ph]].

[46] Keyu Lu, Yue-Lin Sming Tsai, Qiang Yuan, and Le Zhang, “*Inelastic Scattering of Dark Matter with Heavy Cosmic Rays*,” [[arXiv:2310.12501](https://arxiv.org/abs/2310.12501) [astro-ph.HE]].

[47] Jin-Wei Wang, Alessandro Granelli, and Piero Ullio, “*Direct Detection Constraints on Blazar-Boosted Dark Matter*,” *Phys. Rev. Lett.* **128** no. 22, (2022) 221104, [[arXiv:2111.13644](https://arxiv.org/abs/2111.13644) [astro-ph.HE]].

[48] Alessandro Granelli, Piero Ullio, and Jin-Wei Wang, “*Blazar-boosted dark matter at Super-Kamiokande*,” *JCAP* **07** no. 07, (2022) 013, [[arXiv:2202.07598](https://arxiv.org/abs/2202.07598) [astro-ph.HE]].

[49] Chen Xia, Chuan-Yang Xing, and Yan-Hao Xu, “*Boosted dark matter from Centaurus A and its detection*,” *JHEP* **03** (2024) 076, [[arXiv:2401.03772](https://arxiv.org/abs/2401.03772) [hep-ph]].

[50] Yongsoo Jho, Jong-Chul Park, Seong Chan Park, and Po-Yan Tseng, “*Cosmic-Neutrino-Boosted Dark Matter (ν BDM)*,” [[arXiv:2101.11262](https://arxiv.org/abs/2101.11262) [hep-ph]].

[51] Anirban Das and Manibrata Sen, “*Boosted dark matter from diffuse supernova neutrinos*,” *Phys. Rev. D* **104** no. 7, (2021) 075029, [[arXiv:2104.00027](https://arxiv.org/abs/2104.00027) [hep-ph]].

[52] Wei Chao, Tong Li, and Jiajun Liao, “*Connecting Primordial Black Hole to boosted sub-GeV Dark Matter through neutrino*,” [[arXiv:2108.05608](https://arxiv.org/abs/2108.05608) [hep-ph]].

[53] Yen-Hsun Lin, Wen-Hua Wu, Meng-Ru Wu, and Henry Tsui-King Wong, “*Searching for Afterglow: Light Dark Matter Boosted by Supernova Neutrinos*,” *Phys. Rev. Lett.* **130** no. 11, (2023) 111002, [[arXiv:2206.06864](https://arxiv.org/abs/2206.06864) [hep-ph]].

[54] Anirban Das, Tim Herbermann, Manibrata Sen, and Volodymyr Takhistov, “*Energy-dependent Boosted Dark Matter from Diffuse Supernova Neutrino Background*,” [[arXiv:2403.15367](https://arxiv.org/abs/2403.15367) [hep-ph]].

[55] Haipeng An, Maxim Pospelov, Josef Pradler, and Adam Ritz, “*Directly Detecting MeV-scale Dark Matter via Solar Reflection*,” *Phys. Rev. Lett.* **120** no. 14, (2018) 141801, [[arXiv:1708.03642](https://arxiv.org/abs/1708.03642) [hep-ph]]. [Erratum: *Phys. Rev. Lett.* 121, 259903 (2018)].

[56] Timon Emken, “*Solar reflection of light dark matter with heavy mediators,*” *Phys. Rev. D* **105** no. 6, (2022) 063020, [[arXiv:2102.12483](https://arxiv.org/abs/2102.12483) [hep-ph]].

[57] Haipeng An, Haoming Nie, Maxim Pospelov, Josef Pradler, and Adam Ritz, “*Solar reflection of dark matter,*” *Phys. Rev. D* **104** no. 10, (2021) 103026, [[arXiv:2108.10332](https://arxiv.org/abs/2108.10332) [hep-ph]].

[58] Joachim Kopp, Jia Liu, and Xiao-Ping Wang, “*Boosted Dark Matter in IceCube and at the Galactic Center,*” *JHEP* **04** (2015) 105, [[arXiv:1503.02669](https://arxiv.org/abs/1503.02669) [hep-ph]].

[59] Atri Bhattacharya, Raj Gandhi, Aritra Gupta, and Satyanarayan Mukhopadhyay, “*Boosted Dark Matter and its implications for the features in IceCube HESE data,*” *JCAP* **05** (2017) 002, [[arXiv:1612.02834](https://arxiv.org/abs/1612.02834) [hep-ph]].

[60] Kaustubh Agashe, Yanou Cui, Lina Necib, and Jesse Thaler, “*(In)direct Detection of Boosted Dark Matter,*” *JCAP* **10** (2014) 062, [[arXiv:1405.7370](https://arxiv.org/abs/1405.7370) [hep-ph]].

[61] Roberta Calabrese, Marco Chianese, Damiano F. G. Fiorillo, and Ninetta Saviano, “*Direct detection of light dark matter from evaporating primordial black holes,*” *Phys. Rev. D* **105** no. 2, (2022) L021302, [[arXiv:2107.13001](https://arxiv.org/abs/2107.13001) [hep-ph]].

[62] James Alvey, Miguel Campos, Malcolm Fairbairn, and Tevong You, “*Detecting Light Dark Matter via Inelastic Cosmic Ray Collisions,*” *Phys. Rev. Lett.* **123** (2019) 261802, [[arXiv:1905.05776](https://arxiv.org/abs/1905.05776) [hep-ph]].

[63] Liangliang Su, Wenyu Wang, Lei Wu, Jin Min Yang, and Bin Zhu, “*Atmospheric Dark Matter and Xenon1T Excess,*” *Phys. Rev. D* **102** no. 11, (2020) 115028, [[arXiv:2006.11837](https://arxiv.org/abs/2006.11837) [hep-ph]].

[64] Carlos A. Argüelles, Víctor Muñoz, Ian M. Shoemaker, and Volodymyr Takhistov, “*Hadrophilic light dark matter from the atmosphere,*” *Phys. Lett. B* **833** (2022) 137363, [[arXiv:2203.12630](https://arxiv.org/abs/2203.12630) [hep-ph]].

[65] **PandaX** Collaboration, Xuyang Ning et al., “*Search for Light Dark Matter from the Atmosphere in PandaX-4T,*” *Phys. Rev. Lett.* **131** no. 4, (2023) 041001, [[arXiv:2301.03010](https://arxiv.org/abs/2301.03010) [hep-ex]].

[66] E. G. Adelberger et al., “*Solar fusion cross sections II: the pp chain and CNO cycles,*” *Rev. Mod. Phys.* **83** (2011) 195, [[arXiv:1004.2318](https://arxiv.org/abs/1004.2318) [nucl-ex]].

[67] Johannes Bergstrom, M. C. Gonzalez-Garcia, Michele Maltoni, Carlos Peña-Garay, Aldo M. Serenelli, and Ningqiang Song, “*Updated determination of the solar neutrino fluxes from solar neutrino data,*” *JHEP* **03** (2016) 132, [[arXiv:1601.00972](https://arxiv.org/abs/1601.00972) [hep-ph]].

[68] Núria Vinyoles, Aldo M. Serenelli, Francesco L. Villante, Sarbani Basu, Johannes Bergström, M. C. Gonzalez-Garcia, Michele Maltoni, Carlos Peña Garay, and Ningqiang Song, “*A new Generation of Standard Solar Models,*” *Astrophys. J.* **835** no. 2, (2017) 202, [[arXiv:1611.09867](https://arxiv.org/abs/1611.09867) [astro-ph.SR]].

[69] **CAST** Collaboration, S. Andriamonje et al., “*Search for solar axion emission from ^7Li and $D(p, \gamma)^3\text{He}$ nuclear decays with the CAST γ -ray calorimeter,*” *JCAP* **03** (2010) 032, [[arXiv:0904.2103](https://arxiv.org/abs/0904.2103) [hep-ex]].

[70] **Borexino** Collaboration, G. Bellini et al., “*Search for Solar Axions Produced in $p(d, ^3\text{He})\text{A}$ Reaction with Borexino Detector,*” *Phys. Rev. D* **85** (2012) 092003, [[arXiv:1203.6258](https://arxiv.org/abs/1203.6258) [hep-ex]].

[71] Agaman Bhusal, Nick Houston, and Tianjun Li, “*Searching for Solar Axions Using Data from the Sudbury Neutrino Observatory,*” *Phys. Rev. Lett.* **126** no. 9, (2021) 091601, [[arXiv:2004.02733](https://arxiv.org/abs/2004.02733) [hep-ph]].

[72] John D. Vergados, Paraskevi C. Divari, and Hiroyasu Ejiri, “*Calculated Event Rates for Axion Detection via Atomic and Nuclear Processes,*” *Adv. High Energy Phys.* **2022** (2022) 7373365, [[arXiv:2104.12213](https://arxiv.org/abs/2104.12213) [hep-ph]].

[73] C.A. Bertulani and P. Danielewicz, *Introduction to Nuclear Reactions*. CRC Press, 2019.

[74] C. A. Bertulani, “*RADCAP: A Potential model tool for direct capture reactions,*” *Comput. Phys. Commun.* **156** (2003) 123–141, [[arXiv:nucl-th/0305099](https://arxiv.org/abs/nucl-th/0305099)].

[75] J. T. Huang, C. A. Bertulani, and V. Guimaraes, “*Radiative capture of nucleons at astrophysical energies with single-particle states,*” *Atom. Data Nucl. Data Tabl.* **96** (2010) 824–847, [[arXiv:0810.3867](https://arxiv.org/abs/0810.3867) [nucl-th]].

[76] Steven Weinberg, *The Quantum theory of fields. Vol. 1: Foundations*. Cambridge University Press, 6, 2005.

[77] Shao-Feng Ge, Pedro Pasquini, and Jie Sheng, “*Solar active-sterile neutrino conversion with atomic effects at dark matter direct detection experiments,*” *JHEP* **05** (2022) 088, [[arXiv:2112.05560](https://arxiv.org/abs/2112.05560) [hep-ph]].

[78] Jun John Sakurai and Jim Napolitano, *Modern Quantum Mechanics*. Quantum physics, quantum information and quantum computation. Cambridge University Press, 10, 2020.

[79] I. I. Sobel’Man, *Introduction to the Theory of Atomic Spectra*. Elsevier, 2016.

[80] Roger D. Woods and David S. Saxon, “*Diffuse Surface Optical Model for Nucleon-Nuclei Scattering,*” *Phys. Rev.* **95** (1954) 577–578.

[81] David Gaspard, “*Connection formulas between Coulomb wave functions,*” *J. Math. Phys.* **59** (2018) 112104, [[arXiv:1804.10976](https://arxiv.org/abs/1804.10976) [math-ph]].

[82] Claude Cohen-Tannoudji, Bernard Diu, and Franck Laloë, *Quantum Mechanics*, Volume 1 and 2. Wiley-VCH, 2nd ed., 1991. ISBN 978-0471164333 (Vol.1), 978-0471164357 (Vol.2).

[83] International Atomic Energy Agency, “*LiveChart of Nuclides – Advanced Version.*” <https://www-nds.iaea.org/relnsd/vcharthtml/VChartHTML.html>.

[84] Edward W. Kolb and Michael S. Turner, *The Early Universe*, vol. 69. Taylor and Francis, 5, 2019.

[85] Carlos A. Bertulani, *Nuclear Physics in a Nutshell*. Princeton University Press, 4, 2007.

[86] Glenn D. Starkman, Andrew Gould, Rahim Esmailzadeh, and Savas Dimopoulos, “*Opening the Window on Strongly Interacting Dark Matter,*” *Phys. Rev. D* **41** (1990) 3594.

[87] Bradley J. Kavanagh, “*Earth scattering of superheavy dark matter: Updated constraints from detectors old and new,*” *Phys. Rev. D* **97** no. 12, (2018) 123013, [[arXiv:1712.04901](https://arxiv.org/abs/1712.04901) [hep-ph]].

[88] J. I. Collar and F. T. Avignone, “*Diurnal modulation effects in cold dark matter experiments,*” *Phys. Lett. B* **275** (1992) 181–185.

[89] M. Shafi Mahdawi and Glennys R. Farrar, “*Closing the window on $\sim\text{GeV}$ Dark Matter with moderate ($\sim\mu\text{b}$) interaction with nucleons,*” *JCAP* **12** (2017) 004, [[arXiv:1709.00430](https://arxiv.org/abs/1709.00430) [hep-ph]].

[90] Yifan Chen, Bartosz Fornal, Pearl Sandick, Jing Shu, Xiao Xue, Yue Zhao, and Junchao Zong, “*Earth Shielding and Daily Modulation from Electrophilic Boosted Dark Matter,*” [[arXiv:2110.09685](https://arxiv.org/abs/2110.09685) [hep-ph]].

[91] **CDEX** Collaboration, Z. Z. Liu et al., “*Studies of the Earth shielding effect to direct dark matter searches at*

the China Jinping Underground Laboratory,” Phys. Rev. D **105** no. 5, (2022) 052005, [[arXiv:2111.11243](https://arxiv.org/abs/2111.11243) [hep-ex]].

[92] Christopher V. Cappiello, “*Analytic Approach to Light Dark Matter Propagation,”* Phys. Rev. Lett. **130** no. 22, (2023) 221001, [[arXiv:2301.07728](https://arxiv.org/abs/2301.07728) [hep-ph]].

[93] Richard W. Lindquist, “*Relativistic transport theory,”* Annals Phys. **37** no. 3, (1966) 487–518.

[94] Yong Du, Fei Huang, Hao-Lin Li, Yuan-Zhen Li, and Jiang-Hao Yu, “*Revisiting dark matter freeze-in and freeze-out through phase-space distribution,”* JCAP **04** no. 04, (2022) 012, [[arXiv:2111.01267](https://arxiv.org/abs/2111.01267) [hep-ph]].

[95] Chen Xia and Chuan-Yang Xing, “*DarkProp-v0.3.*” <http://yfzhou.itp.ac.cn/darkprop>, 2024.

[96] XENON Collaboration, E. Aprile et al., “*Light Dark Matter Search with Ionization Signals in XENON1T,”* Phys. Rev. Lett. **123** no. 25, (2019) 251801, [[arXiv:1907.11485](https://arxiv.org/abs/1907.11485) [hep-ex]].

[97] PandaX Collaboration, Shuaijie Li et al., “*Search for Light Dark Matter with Ionization Signals in the PandaX-4T Experiment,”* Phys. Rev. Lett. **130** no. 26, (2023) 261001, [[arXiv:2212.10067](https://arxiv.org/abs/2212.10067) [hep-ex]].

[98] DarkSide-50 Collaboration, P. Agnes et al., “*Search for low-mass dark matter WIMPs with 12 ton-day exposure of DarkSide-50,”* Phys. Rev. D **107** no. 6, (2023) 063001, [[arXiv:2207.11966](https://arxiv.org/abs/2207.11966) [hep-ex]].

[99] DarkSide Collaboration, P. Agnes et al., “*Search for Dark-Matter–Nucleon Interactions via Migdal Effect with DarkSide-50,”* Phys. Rev. Lett. **130** no. 10, (2023) 101001, [[arXiv:2207.11967](https://arxiv.org/abs/2207.11967) [hep-ex]].

[100] Global Argon Dark Matter Collaboration, P. Agnes et al., “*Sensitivity projections for a dual-phase argon TPC optimized for light dark matter searches through the ionization channel,”* Phys. Rev. D **107** no. 11, (2023) 112006, [[arXiv:2209.01177](https://arxiv.org/abs/2209.01177) [physics.ins-det]].

[101] PandaX-II Collaboration, Xiangyi Cui et al., “*Search for Cosmic-Ray Boosted Sub-GeV Dark Matter at the PandaX-II Experiment,”* Phys. Rev. Lett. **128** no. 17, (2022) 171801, [[arXiv:2112.08957](https://arxiv.org/abs/2112.08957) [hep-ex]].

[102] Super-Kamiokande Collaboration, K. Abe et al., “*Search for Cosmic-Ray Boosted Sub-GeV Dark Matter Using Recoil Protons at Super-Kamiokande,”* Phys. Rev. Lett. **130** no. 3, (2023) 031802, [[arXiv:2209.14968](https://arxiv.org/abs/2209.14968) [hep-ex]]. [Erratum: Phys. Rev. Lett. 131, 159903 (2023)].

[103] SENSEI Collaboration, Prakruth Adari et al., “*SENSEI: First Direct-Detection Results on sub-GeV Dark Matter from SENSEI at SNOLAB,”* [[arXiv:2312.13342](https://arxiv.org/abs/2312.13342) [astro-ph.CO]].

[104] Zurab Berezhiani, Aleksander Dolgov, and Igor Tkachev, “*BBN with light dark matter,”* JCAP **02** (2013) 010, [[arXiv:1211.4937](https://arxiv.org/abs/1211.4937) [astro-ph.CO]].

[105] Kenneth M. Nollett and Gary Steigman, “*BBN And The CMB Constrain Light, Electromagnetically Coupled WIMPs,”* Phys. Rev. D **89** no. 8, (2014) 083508, [[arXiv:1312.5725](https://arxiv.org/abs/1312.5725) [astro-ph.CO]].

[106] Daniel Green and Surjeet Rajendran, “*The Cosmology of Sub-MeV Dark Matter,”* JHEP **10** (2017) 013, [[arXiv:1701.08750](https://arxiv.org/abs/1701.08750) [hep-ph]].

[107] Gordan Krnjaic and Samuel D. McDermott, “*Implications of BBN Bounds for Cosmic Ray Upscattered Dark Matter,”* Phys. Rev. D **101** no. 12, (2020) 123022, [[arXiv:1908.00007](https://arxiv.org/abs/1908.00007) [hep-ph]].

[108] Nashwan Sabti, James Alvey, Miguel Escudero, Malcolm Fairbairn, and Diego Blas, “*Refined Bounds on MeV-scale Thermal Dark Sectors from BBN and the CMB,”* JCAP **01** (2020) 004, [[arXiv:1910.01649](https://arxiv.org/abs/1910.01649) [hep-ph]].

[109] Rui An, Vera Gluscevic, Erminia Calabrese, and J. Colin Hill, “*What does cosmology tell us about the mass of thermal-relic dark matter?,*” JCAP **07** no. 07, (2022) 002, [[arXiv:2202.03515](https://arxiv.org/abs/2202.03515) [astro-ph.CO]].

[110] Jared A. Evans, Akshay Ghalsasi, Stefania Gori, Michele Tammaro, and Jure Zupan, “*Light Dark Matter from Entropy Dilution,”* JHEP **02** (2020) 151, [[arXiv:1910.06319](https://arxiv.org/abs/1910.06319) [hep-ph]].

[111] P. F. de Salas, M. Lattanzi, G. Mangano, G. Miele, S. Pastor, and O. Pisanti, “*Bounds on very low reheating scenarios after Planck,”* Phys. Rev. D **92** no. 12, (2015) 123534, [[arXiv:1511.00672](https://arxiv.org/abs/1511.00672) [astro-ph.CO]].

[112] Tsung-Han Yeh, Jessie Shelton, Keith A. Olive, and Brian D. Fields, “*Probing physics beyond the standard model: limits from BBN and the CMB independently and combined,”* JCAP **10** (2022) 046, [[arXiv:2207.13133](https://arxiv.org/abs/2207.13133) [astro-ph.CO]].